EasyChair Preprint

№ 1750

Simple multi-legged model reveals that Retrograde-wave gait rather attenuates body oscillation than Direct-wave gait

Yuichi Ambe and Shinya Aoi

October 23, 2019

Simple multi-legged model reveals that Retrograde-wave gait rather attenuates body oscillation than Direct-wave gait

Yuichi Ambe[1†] and Shinya Aoi[2]

[1]Graduate school of engineering, Tohoku University, Sendai, Japan
(Tel: +81-22-795-7025; E-mail: ambe@rm.is.tohoku.ac.jp)
[2]Graduate school of engineering, Kyoto University, Kyoto, Japan

Abstract: Multi-legged animals show mainly two types of ipsilateral interlimb coordination. Millipedes show the direct-wave gait in which the swing leg movements propagate from posterior to anterior, while some centipedes show the retrograde-wave gait in which the swing movements propagate inversely. Centipedes often oscillate their body on horizontal plane as the walking speed gets faster, while millipedes do not show this feature. However, the functional differences between those two gaits are not clear. As the purpose of this study, we investigate whether the retrograde-wave gait rather induces body oscillation than the direct-wave gait as the functional difference using simulation. We model the multi-legged animal by the simple springy multi-link model actuated by external forces on the links. Then we investigate the effect of direct- and retrograde-wave gaits on the body oscillation. Our result shows that the retrograde-wave gait rather attenuates the body oscillation than the direct-wave gait, which contradicts the preference of body oscillation and retrograde-wave gait in centipedes.

Keywords: Multi-legged animal, Direct wave gait, Retrograde wave gait, Interlimb coordination, Body oscillation, Continuum robot

1. INTRODUCTION

Multi-legged animals show several types of ipsilateral interlimb coordination according to situations. Millipedes show the direct wave gait in which the swing leg movements propagate from posterior to anterior [1, 2]. On the other hand, some centipedes show the retrograde wave gait in which the swing movements propagate from anterior to posterior [1, 2]. More interestingly, centipedes often oscillates their body on horizontal plane as walking speed gets faster [3], while millipedes do not show these features.

The functional differences of those two gaits are not clear although there are several studies which discuss those two gaits. Direct and retrograde waves are also observed in peristalsis [4]. Researchers pointed out that the mechanical features of direct and retrograde wave gaits of multi-legged animals are related to these in peristalsis [2]. The other researchers show that direct-wave gait is more stable in terms of perturbation resistance than retrograde-wave gait in the case of six-legged robot model [5]. If the functional roles of the two gaits are explained, it would contribute to not only understanding the animal but also giving clues for designing the multi-legged robots.

As the purpose of this study, we investigate whether the retrograde-wave gait rather induces body oscillation than the direct-wave gait as the functional difference using simulation. Millipedes walk using the direct-wave gait while there is not severe body vibration. On the other hand, some centipedes walk using retrograde-wave gait while the body largely oscillates horizontally. From these facts, we expect that the direct-wave gait hardly induces body oscillation while the retrograde-wave gait is more likely to induce body oscillation. In order to investigate the expectation, we take a minimal modelling approach. We model the flexible torso of multi-legged animals using a simple multi-link model whose links are connected by passive rotary springs. The driving force obtained by the movement of the leg is modelled as a periodic external force applied to the link. Phase differences of forces between links represent the direction of swing movement. Then, a simulation is conducted to investigate how the behaviour of the flexible body changes due to the direct- and retrograde-waves.

† Yuichi Ambe is the presenter of this paper.

2. SIMPLE MODEL

2.1. Assumption and model

In this study, we construct a flexible continuum robot model (Fig. 1) based on the following assumptions with reference to real multi-legged animals.

- *(A1)* Multi-legged animals crawl on the ground and make the body meander laterally. In this model, the motion is analysed on a horizontal plane for simplicity.
- *(A2)* Multi-legged animals have flexible torso, and dominant body oscillations seem lower order. We approximate the flexible torso using multi-body model for simplicity. Each element i is modelled as a rigid link i and connected by joint with rotating spring and damper. The neutral angle of the rotating spring is 0 [rad].
- *(A3)* The driving force obtained by moving a leg of multi-legged animals is approximated by the periodical external force acting on the center of mass (COM) of link i. Suppose that the force f_i is exerted along the longitudinal axis of the link.
- *(A4)* The friction between multi-legged animals and the environment is modelled as a viscous drag force which is proportional to the velocity of the COM of

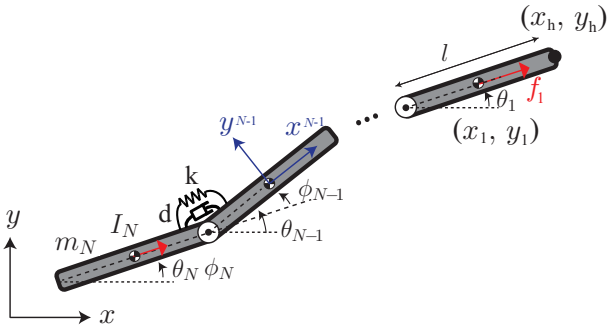

Fig. 1 Model of multi-legged animals.

each link. We set the viscous coefficient in the longitudinal direction of the link as c_x and that of vertical direction as c_y.

Under the above assumptions, the model consists of N rigid links (mass: $m_i > 0$, inertia moment: $I_i > 0$, length: $l > 0$) connected by elastic joints (spring constant:k, damper constant:d) in the $O-xy$ plane. The head link is link 1. For link i, we denote the pitch angle by θ_i, joint angle by ϕ_i, COM position (the center of the link) by (x_i, y_i), the head position by (x_h, y_h) and external force on the COM along longitudinal axis by f_i. We set the axes on each link i as x^i, y^i as shown in Fig. 1. The gravity acceleration, viscous coefficients along x^i and y^i axes are defined as g, c_x and c_y, respectively. From here, for simplification of the derivation, we define the vectors $\boldsymbol{x}, \boldsymbol{y}, \boldsymbol{\theta}, \boldsymbol{m}, \boldsymbol{\phi}$ and $\boldsymbol{f} \in R^{N\times 1}$ whose elements are $x_i, y_i, \theta_i, m_i, \phi_i$ and f_i $(i = 1, \ldots, N)$, respectively. The general coordinate of the system is defined as $\boldsymbol{q} = [x_h\ y_h\ \boldsymbol{\theta}^T]^T$.

2.2. Equation of motion

Equation of motion can be derived as follows referring the paper [6]. We omit the detailed derivation because the procedure is similar to that of [6].

$$H\ddot{\boldsymbol{q}} + \left(J_{qx}^T M J_x + J_{qy}^T M J_y\right) \mathrm{diag}(\dot{\boldsymbol{q}})\dot{\boldsymbol{q}} + C\dot{\boldsymbol{q}} + K\boldsymbol{q} = J_{qx}^T C_\theta \boldsymbol{f} + J_{qy}^T S_\theta \boldsymbol{f} \quad (1)$$

where

$$\begin{aligned} C_\theta &\equiv \mathrm{diag}(\cos\theta_1, \ldots, \cos\theta_N), \\ S_\theta &\equiv \mathrm{diag}(\sin\theta_1, \ldots, \sin\theta_N) \\ J_{qx} &= [\boldsymbol{e}\ \boldsymbol{0}\ lAS_\theta], J_x = [\boldsymbol{0}\ \boldsymbol{0}\ lAC_\theta] \\ J_{qy} &= [\boldsymbol{0}\ \boldsymbol{e}\ -lAC_\theta], J_y = [\boldsymbol{0}\ \boldsymbol{0}\ lAS_\theta] \\ H &= J_{qx}^T M J_{qx} + J_{qy}^T M J_{qy} + J_{q\theta}^T I J_{q\theta} \\ K &= kJ_{q\theta}^T R^T R J_{q\theta}, J_{q\theta} = [\boldsymbol{0}\ \boldsymbol{0}\ E] \end{aligned}$$

$$\begin{aligned} C &= dJ_{q\theta}^T R^T R J_{q\theta} \\ &+ \begin{bmatrix} J_{qx} \\ J_{qy} \end{bmatrix}^T \begin{bmatrix} c_x C_\theta^2 + c_y S_\theta^2 & (c_x - c_y) C_\theta S_\theta \\ (c_x - c_y) C_\theta S_\theta & c_x S_\theta^2 + c_y C_\theta^2 \end{bmatrix} \begin{bmatrix} J_{qx} \\ J_{qy} \end{bmatrix} \end{aligned}$$

Table 1 **Physical parameters for the simulation.**

Element	Value	Element	Value	Element	Value
N	10	k^*	1.0	c_x^*	0.50
m_{1-10}^*	1.0	d^*	0.50	c_y^*	10
I_{1-10}^*	0.15				

Note that $\boldsymbol{e} = [1\ 1\ \ldots\ 1]^T \in R^{N\times 1}, E \in R^{N\times N}$ is identity matrix, matrix R fulfils $\boldsymbol{\phi} = R\boldsymbol{\theta}$ and

$$A = \begin{bmatrix} 1/2 & 0 & \ldots & 0 \\ 1 & 1/2 & \ldots & 0 \\ \vdots & \vdots & \ddots & \vdots \\ 1 & 1 & \ldots & 1/2 \end{bmatrix}$$

3. SIMULATION

3.1. dimensionless equation and physical parameters

To reduce the parameters to investigate, m, l, and $\sqrt{l/g}$ are used as the characteristic mass, length, and time scale of the model, respectively. The variables are made dimensionless as $m_i^* = m_i/m$, $I_i^* = I_i/(ml^2)$, $k^* = k/(lmg)$, $d^* = d/(lm\sqrt{lg})$, $f_i^* = f_i/(mg)$, $\dot{()}^* = \sqrt{l/g}\dot{()}$, $\theta^* = \theta$, $t^* = t\sqrt{g/l}$. Then, the dimensionless equation of motion is derived by dividing (1) by lmg.

We set the dimensionless parameter as shown in Table 1. The inertia moment is set as small value compared with the mass of the link. The viscous coefficient for the vertical direction of the link c_y^* is set as large value because the legged-animal does not move side direction in walking.

3.2. Simulation setup

For the simulation, we input three types of force inputs: the constant input $f_i = 1.1$, the sinusoidal function representing a direct-wave gait as

$$f_i^* = 1.1 \sin\left(\frac{\pi}{3}t^* + \frac{2i\pi}{10}\right) + 1.1$$

and the sinusoidal function representing a retrograde-wave gait as

$$f_i^* = 1.1 \sin\left(\frac{\pi}{3}t^* - \frac{2i\pi}{10}\right) + 1.1.$$

Note that the each force input oscillates periodically in a period 6, and a peak of force input propagates forward and backward with the phase difference $\pi/5$. Then we numerically calculate the equation of motion (1) by using *ODE45* function of *MATLAB*. We set the initial state values at $t^* = 0$ as $\boldsymbol{q}^* = [0\ 0\ 0.01\ 0.01\ \ldots 0.01]^T$ and $\dot{\boldsymbol{q}}^* = \boldsymbol{0}$.

3.3. Simulation result

The time responses of ϕ_1, ϕ_5 and ϕ_9 for above three force inputs are shown in Fig. 2. Figures A, B and C correspond to the cases of the constant force, the force input

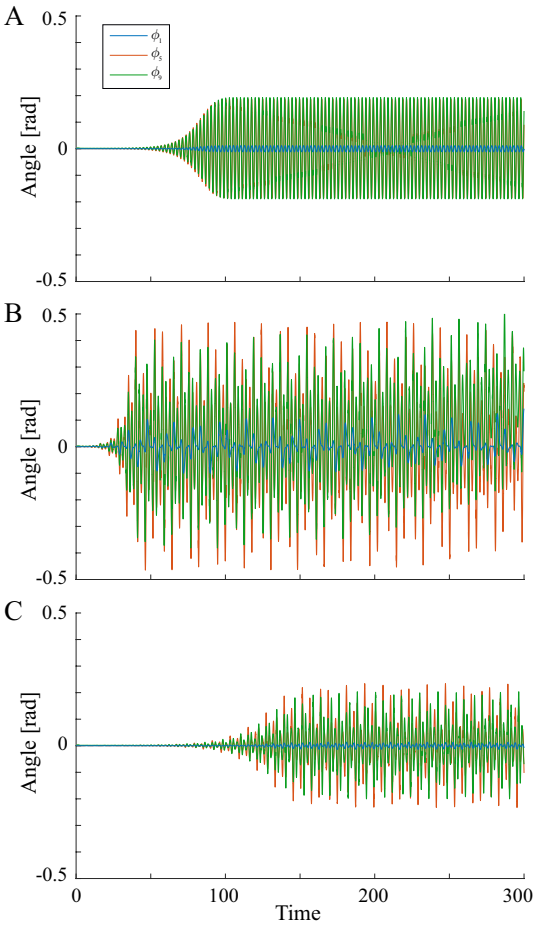

Fig. 2 Time responses of ϕ_1, ϕ_5 and ϕ_9 for the three force inputs (A: constant force input, B: force input imitating direct-wave gait and C: force input imitating retrograde-wave gait)

of direct-wave gait and the force input of retrograde-wave gait, respectively. From Fig. 2A, even when the force input is constant, the body shape start oscillation as time goes by. In the case of direct-wave gait (Fig. 2B), the body starts oscillation fastest in the three. In addition, the amplitude of the body oscillation is twice larger than that of constant force input. On the other hand, in the case of retrograde-wave gait (Fig. 2C), the evolution of body oscillation is slowest in the three, and the amplitude is attenuated compared with the case of direct-wave gait.

To investigate the other features for the force inputs, we show the time responses of head velocity $\sqrt{\dot{x}_{\rm h}^2 + \dot{y}_{\rm h}^2}$ in Fig. 3. The meaning of Figures A, B and C is the same as above. From the figure, we find that the retrograde wave gait show the fastest velocity when the body oscillates. The moving velocity is even faster than the case of constant force input. The direct wave gait shows the slowest velocity in the three. We think this is because the severe body oscillation takes away the energy for propelling.

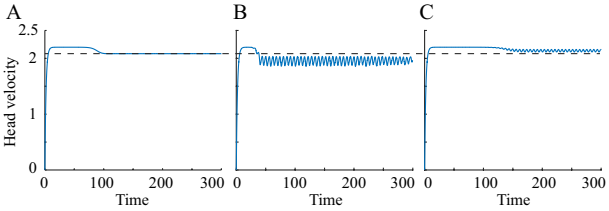

Fig. 3 Time responses of head velocity $\sqrt{\dot{x}_{\rm h}^2 + \dot{y}_{\rm h}^2}$ for the three force inputs (A: constant force input, B: force input imitating direct-wave gait and C: force input imitating retrograde-wave gait)

4. CONCLUSION

We model the multi-legged animal by the simple springy multi-link model actuated by external forces on the links. Then we investigate the effect of direct- and retrograde wave gaits on the body oscillation. Our result shows that the retrograde-wave gait rather attenuates the body oscillation than the direct-wave gait, which does not explain the preference of body oscillation and retrograde-wave gait in centipedes.

In the future, the stability analysis and detailed parameter study will be conducted to generalize the results. In addition, we investigate the differences of these two gaits in terms of other aspects, such as energy efficiency.

ACKNOWLEDGEMENT

This work was supported by JSPS KAKENHI Grant Number JP18K13723.

REFERENCES

[1] R. J. Full, *The Handbook of Comparative Physiology*. Oxford University Press, 1997, ch. Invertebrate locomotor system, pp. 853–930.

[2] S. Kuroda, I. Kunita, Y. Tanaka, A. Ishiguro, R. Kobayashi, and T. Nakagaki, "Common mechanics of mode switching in locomotion of limbless and legged animals," *Journal of The Royal Society Interface*, vol. 11, 20140205, 2014.

[3] S. Aoi, Y. Egi, and K. Tsuchiya, "Instability-based mechanism for body undulations in centipede locomotion," *Physical Review E*, vol. 87, no. 1, 012717, 2013.

[4] Y. Tanaka, K. Ito, T. Nakagaki, and R. Kobayashi, "Mechanics of peristaltic locomotion and role of anchorling," *Journal of The Royal Society Interface*, vol. 9, pp. 222 – 233, 2012.

[5] Y. Ambe, S. Aoi, T. Nachstedt, P. Manoonpong, F. Wörgötter, and F. Matsuno, "Simple analytical model reveals the functional role of embodied sensorimotor interaction in hexapod gaits," *PLOS ONE*, vol. 13, no. 2, e0192469, 2018.

[6] R. Ariizumi and F. Matsuno, "Dynamical analysis of sidewinding locomotion by a snake-like robot," in *2013 IEEE International Conference on Robotics and Automation*, May 2013, pp. 5149–5154.